Regional differences in processes controlling Arctic sea ice floe size distribution in Chukchi Sea, East Siberian and Fram Strait during pre-ponding season

Yanan Wang* (1), Byongjun Hwang (1), Rajlaxmi Basu (1), and Jinchang Ren (2)

(1) University of Huddersfield, (2) University of Strathclyde

*1st year PhD candidate Yanan.Wang@hud.ac.uk

NERC SCIENCE OF THE ENVIRONMENT

Introduction: Background & Motivation

- Floe size distribution (FSD) is considered important to understand and model the physical processes in the marginal ice zone (MIZ).
- FSD is controlled by ice advection, thermodynamics (lateral melting), and dynamics (winds, tides, currents and ocean swell).
- The thermodynamic and dynamic conditions are different between the western Arctic (e.g., Chukchi and Beaufort Seas) and the eastern Arctic (e.g., Fram Strait).
- A more detailed analysis is needed to understand how different physical processes may affect FSD in various spatial and temporal scales.
- In this study, we analysed FSD data derived from three locations in the Arctic to investigate the regional differences in FSD and how various physical processes have affected the results of FSD.

Method

- We analysed the FSD data derived from MEDEA images [Kwok and Untersteiner, 2011] in Chukchi Sea (70°N, 170°W), East Siberian Sea (82°N, 150°E) and Fram Strait (84.9°N, 0.5°E). MEDEA visible images, the high-resolution remotely sensed data, are collected by MEDEA group. The spatial resolution of the original images is 1 m, but degraded to 2 m in this study for faster processing.
- During pre-ponding period, there are 16 images in the Chukchi Sea, 11 images in the East Siberian Sea and 14 images in the Fram Strait.
- FSD is retrieved by the algorithm described in Hwang et al. (2017)

Figure 1. Bathymetric map of the Arctic Ocean with the three selected sites.

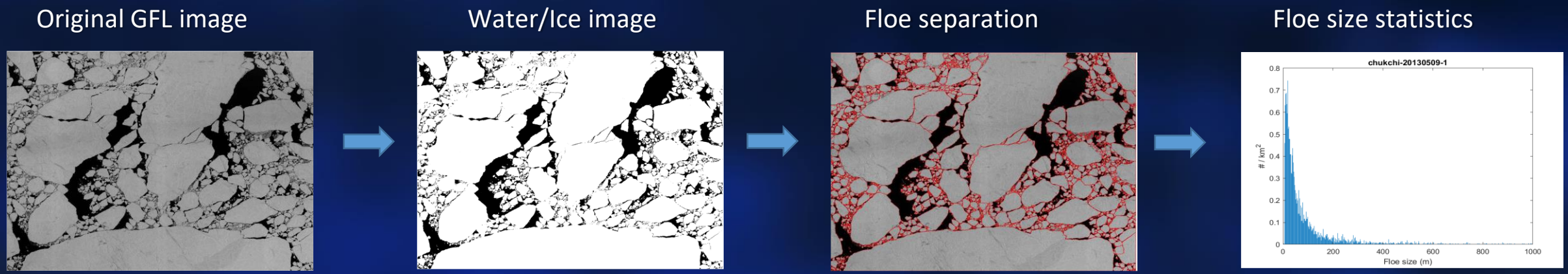

Figure. 2. Retrieval of sea ice floe size distribution (FSD) from satellite imagery.

Method

- Floe number density (FND) follows a power-law relationship as $n(p) = cp^{-\alpha}$, where the exponent α describes the slope of the fit line and the normalization constant c describes the y-intercept [Rothrock and Thorndike, 1984].
- We adapted the Maximum Likelihood Estimate (MLE) developed by Virkar and Clauset, [2014], to calculate the α.
- p-values for the Kolmogorov-Smirnov goodness-of-fit test are shown in Table 1: 7/16 of the data in Chukchi Sea, 6/11 at East Siberian Sea and 8/14 at Fram Strait passed the goodness-of-the fit test (p-value ≥ 0.1).

Chukchi Sea		East Siberian Sea		Fram Strait	
Date	p-value	Date	p-value	Date	p-value
20060517	0.206	20000607	0.102	20000607	0.439
20060524	0.44	20000628	0.013	20010606	0.151
20060604	0.064	20010616	0.005	20010611	0.006
20060612	0.563	20010616	0.002	20010615	0.248
20100530	0.407	20010620	0.115	20010624	0.05
20100530	0	20020701	0.489	20010630	0.027
20110529	0.471	20020701	0.937	20010630	0.335
20120601	0.06	20080531	0.012	20020608	0.697
20130509	0.29	20080609	0.544	20020608	0.069
20130531	0.02	20130613	0.147	20090602	0.434
20140502	0.069	20130706	0.081	20120625	0.193
20140513	0.001			20130605	0.001
20140527	0.017			20130618	0.024
20140527	0.214			20140707	0.216
20140610	0.005				
20140610	0.043				

Table 1. p-value for the Kolmogorov-Smirnov goodness-of-fit test in the three selected sites.

Results 1: Regional characteristics of FSD

Table 2. Power-law exponent α, total floe number density (TFND) in the three selected sites.

Sites	α	TFND (km^{-2})	TFND (km^{-2})	
Chukchi Sea	2.75 ± 0.34	21.28 ± 5.35	d < 100 m	14.01 ± 5.84
			d ≥ 100 m	7.23 ± 1.74
East Siberian Sea	2.46 ± 0.35	10.29 ± 4.24	d < 100 m	5.07 ± 1.96
			d ≥ 100 m	5.16 ± 2.79
Fram Strait	2.46 ± 0.25	7.23 ± 3.57	d < 100 m	3.94 ± 1.93
			d ≥ 100 m	3.23 ± 1.87

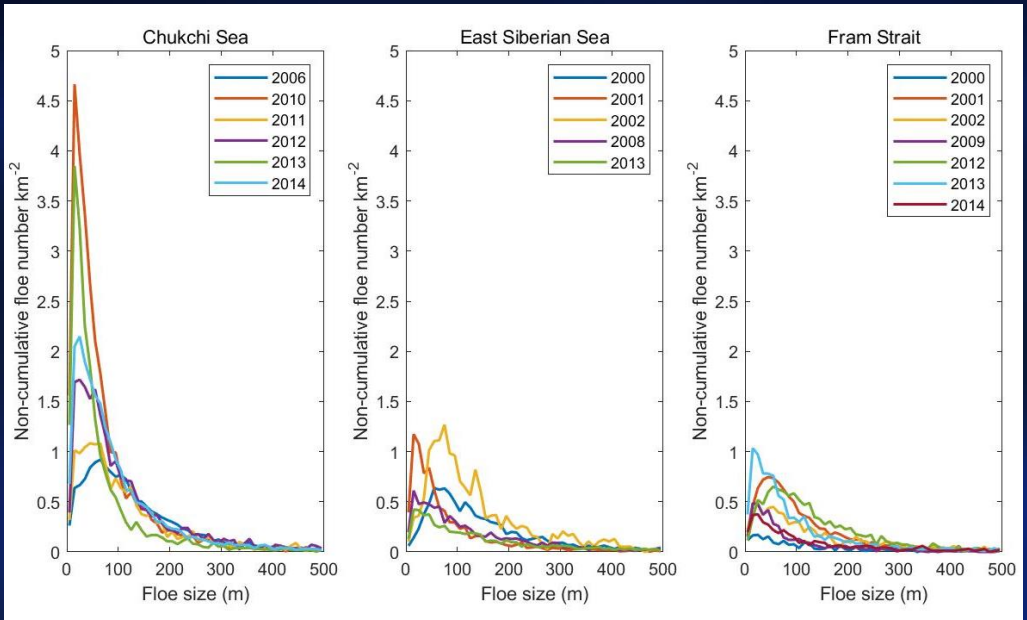

Figure 3. Interannual variability of floe number density (FND) in the three selected sites.

- The power-law exponent α is large in Chukchi Sea (Table 2), indicating a larger percentage of small floes than to the other two sites.
- The total floe number density (TFND) values at Chukchi Sea is the highest (Table 2), where the TFND of small floes is almost twice more than big floes. In other two sites, the TFND of the two floe size groups are almost the same (Table 2).
- In Chukchi Sea, FSD shows larger interannual variability, due mainly to the considerable variability of small floes (Fig 3).
- At Fram Strait and East Siberian Sea, the variability of the FSD is relatively small (Fig 3).

Results 2: Difference of FSD across 2012 in Chukchi Sea

- In the western Arctic (Chukchi Sea and East Siberian), FSD is significantly different across 2012
- In Chukchi Sea, there has been a **23% increase** of small floes.
- In East Siberian Sea, the small floes has **decreased by almost half** after 2012.
- The differences are less evident in the Fram Strait.

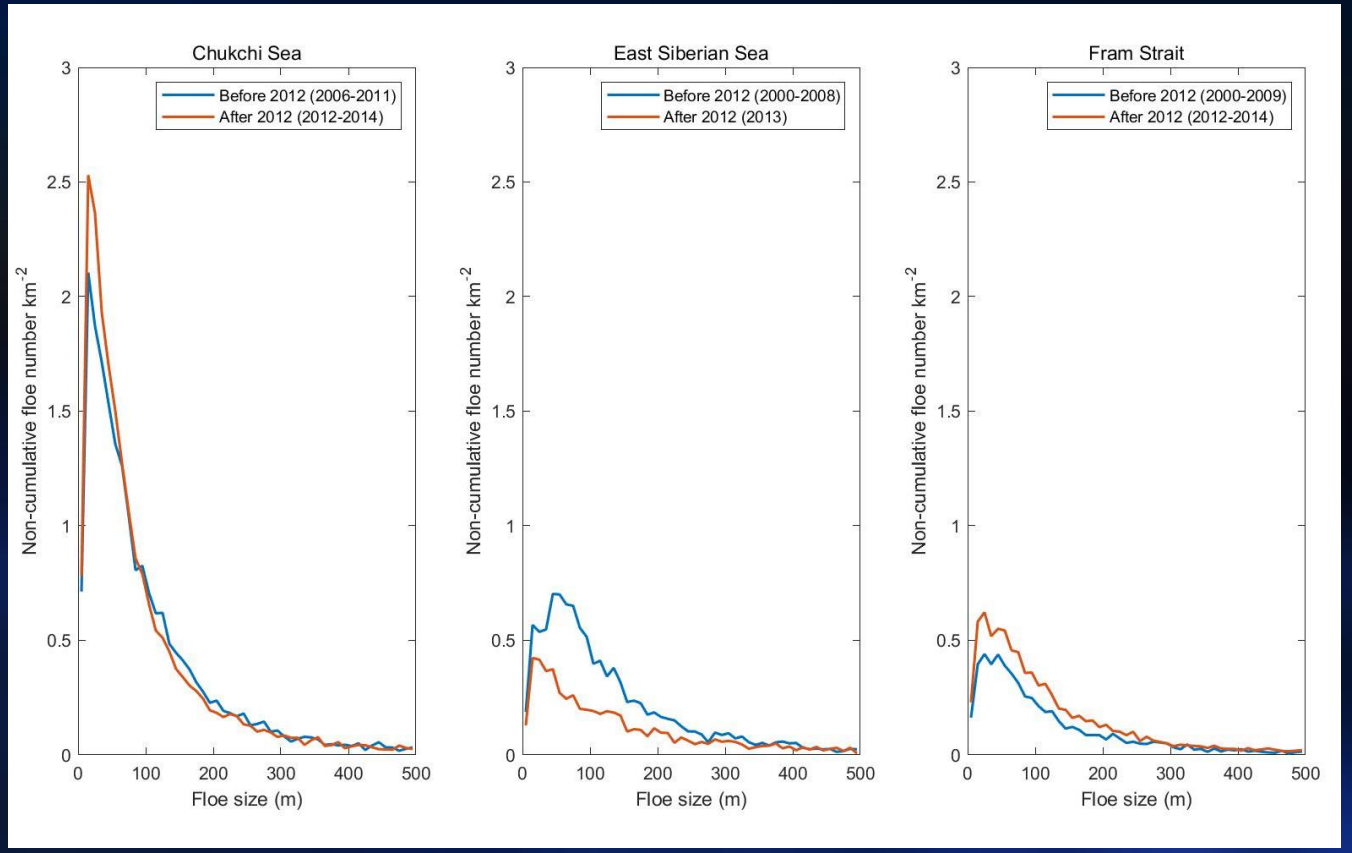

Figure 4. Changes of floe number density (FND) across 2012 at the three selected sites.

Results 3: Processes controlling the change of FSD across 2012

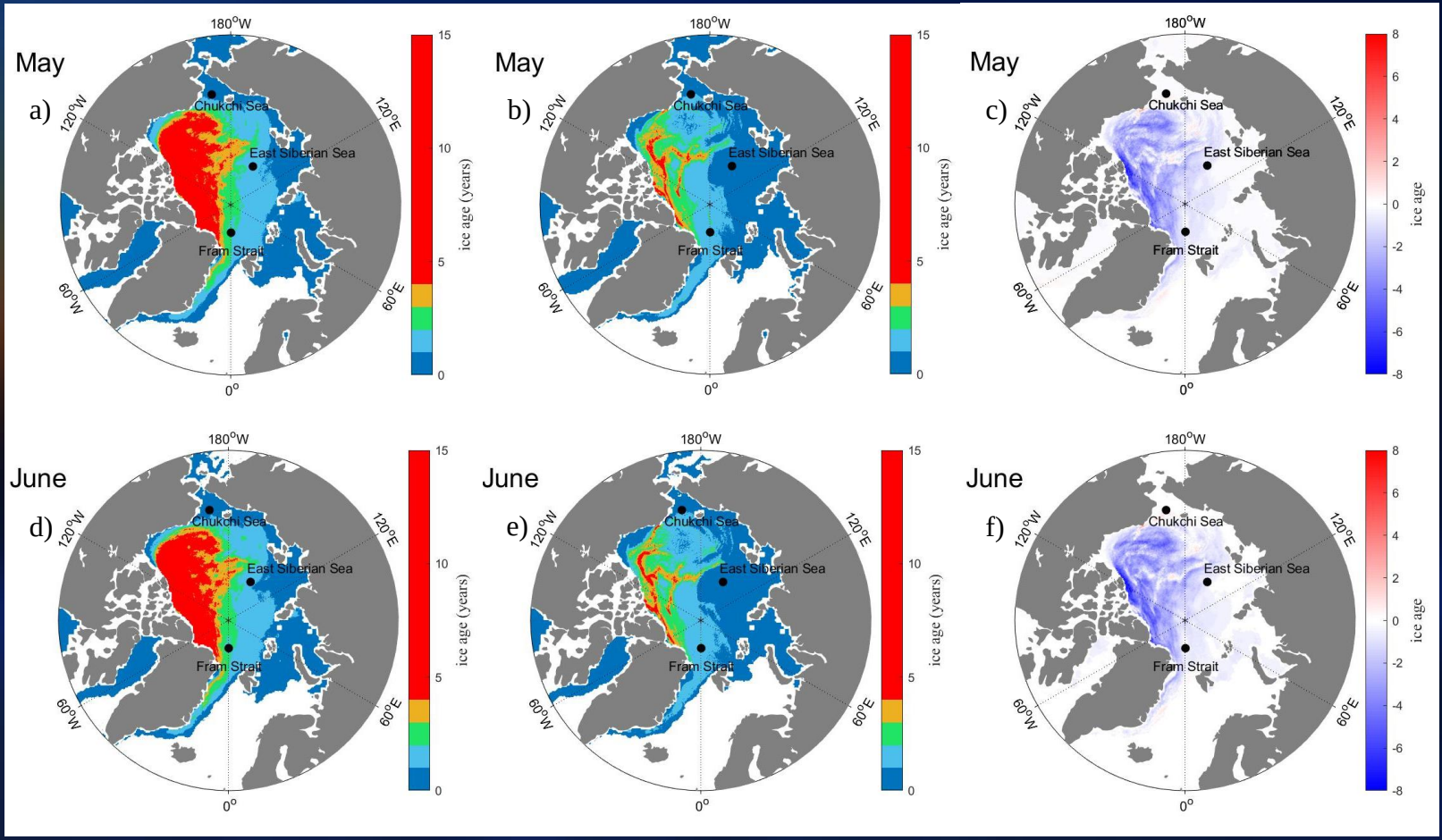

Figure 5. Sea Ice Age in the Arctic. (a) (d) Sea ice age before 2012 (2000-2011); (b) (e) Sea ice age after 2012 (2012-2014) ; (c) (f) The change of sea ice age across 2012. Data for this figure is from EASE-Grid Sea Ice Age, Version 4, at https://nsidc.org/data/NSIDC-0611/versions/4.

- 11/16 pre-ponding images in Chukchi Sea are in May.
- 7/11 and 13/14 pre-ponding images in East Siberian Sea and Fram Strait are in June.
- In Chukchi Sea, there is no significant change of sea ice age in May and June before and after 2012.
- In East Siberian Sea and Fram Strait, the sea ice age tends to be younger.
- The sea ice age is older in East Arctic (Fram Strait) than in West Arctic (Chukchi Sea and East Siberian Sea), i.e. the sea ice in the East Arctic is thicker, stronger and less possible to fracture during the changes in atmospheric and oceanic forcing.

Results 3: Processes controlling the change of FSD across 2012

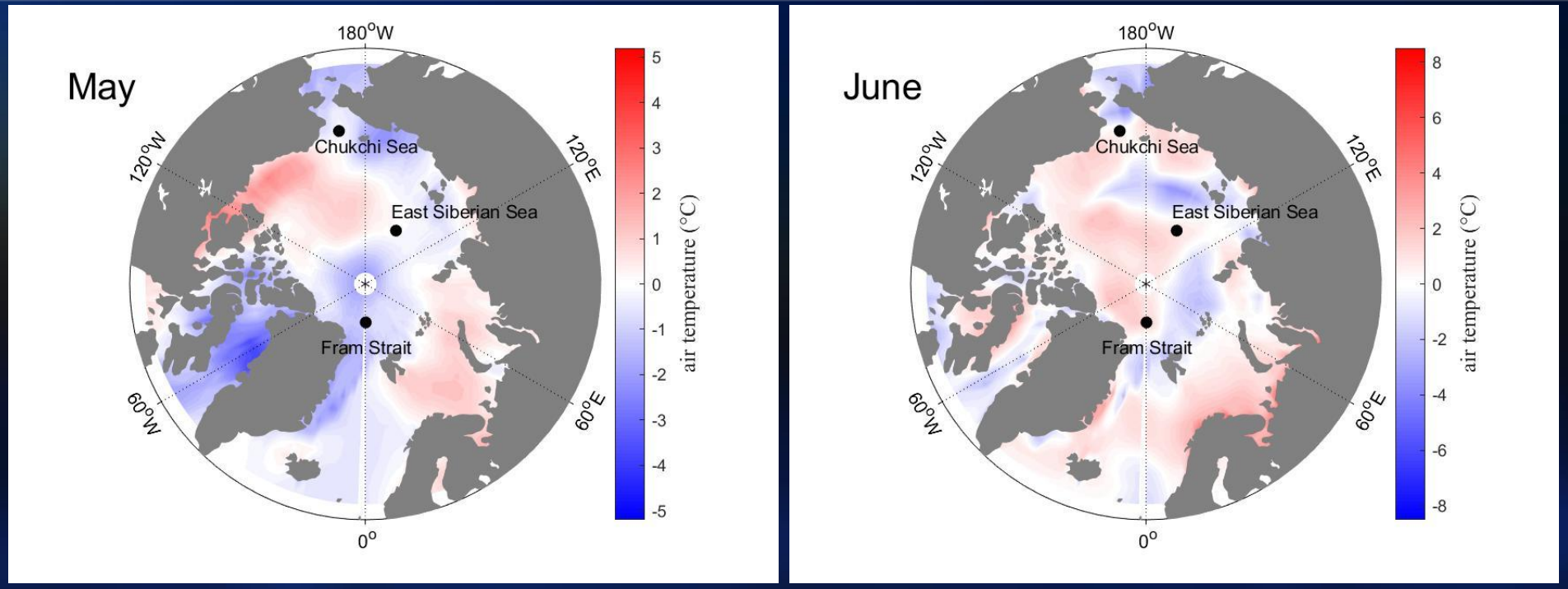

Figure 6. Changes of 2-m air temperature before 2012 (2000-2011) and after 2012 (2012-2014) in May and June.

- In Chukchi Sea, the air temperature slightly decreased by 0.12 ℃ in May and slightly increased by 0.22 ℃ in June across 2012.
- Air temperature increased by about 1.30 ℃ across 2012 in June in East Siberian.
- In Fram Strait, there was a 1.58 ℃ increase of air temperature in June

Results 3: Processes controlling the change of FSD across 2012

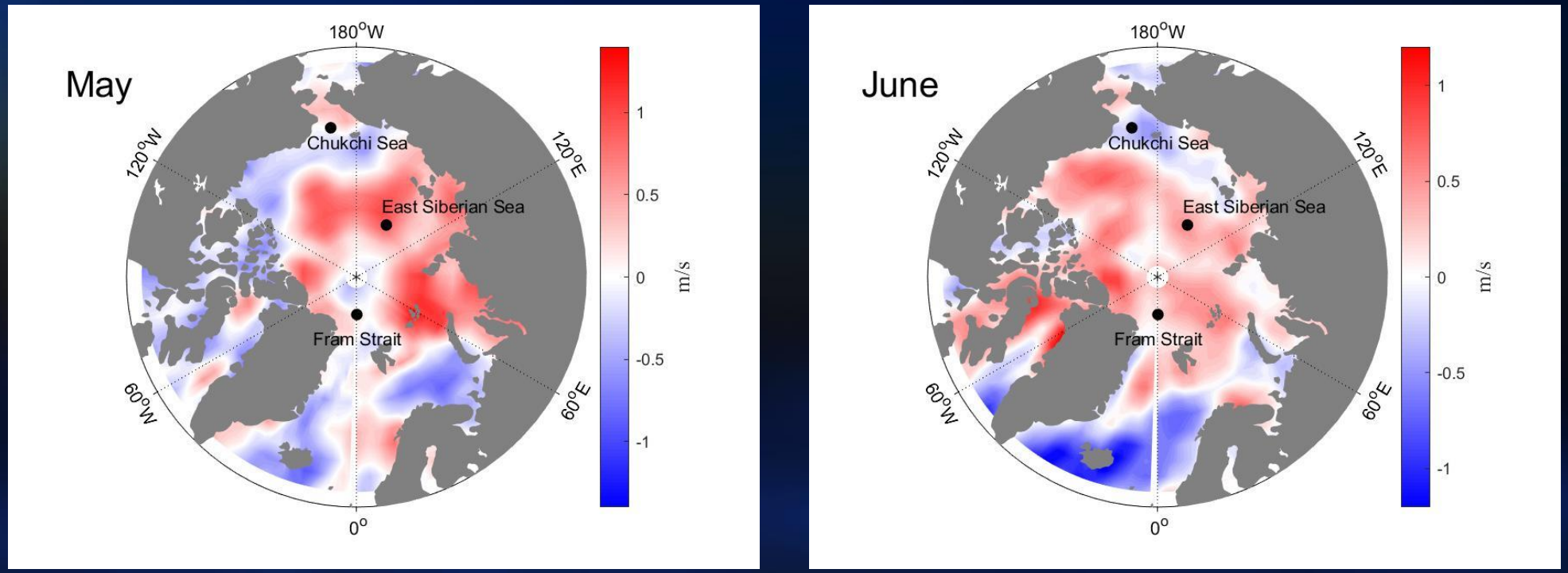

Figure 7. Changes of wind speed before 2012 (2000-2011) and after 2012 (2012-2014) in May and June.

- In Chukchi Sea, the wind speed **increased by 0.18 m/s in May** and **decreased by 0.22 m/s in June across 2012**.
- Wind speed **increase by 0.53 m/s and 0.19 m/s** across 2012 in June in East Siberian and Fram Strait.

Results 4: Processes controlling regional FSD (Chukchi Sea)

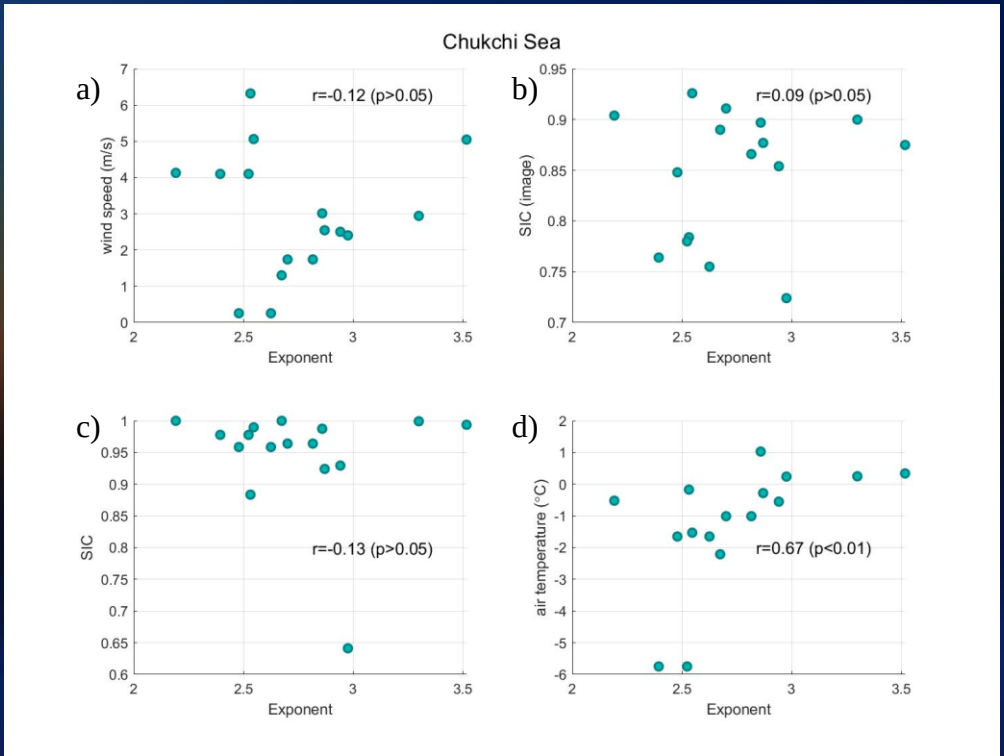

Figure 8. Correlation between the power-law exponent α and wind speed (a), SIC (b and c) and air temperature (d) in Chukchi Sea. Panels (b) is the SIC from MEADEA image (~10 km). Panels (c) shows the daily NOAA/NSIDC SIC data (25km x 25km) in 2012 and daily AMSR-E and AMSR-2 SIC data (6.5km x 6.5km) in 2006, 2010, 2011, 2013 and 2014.

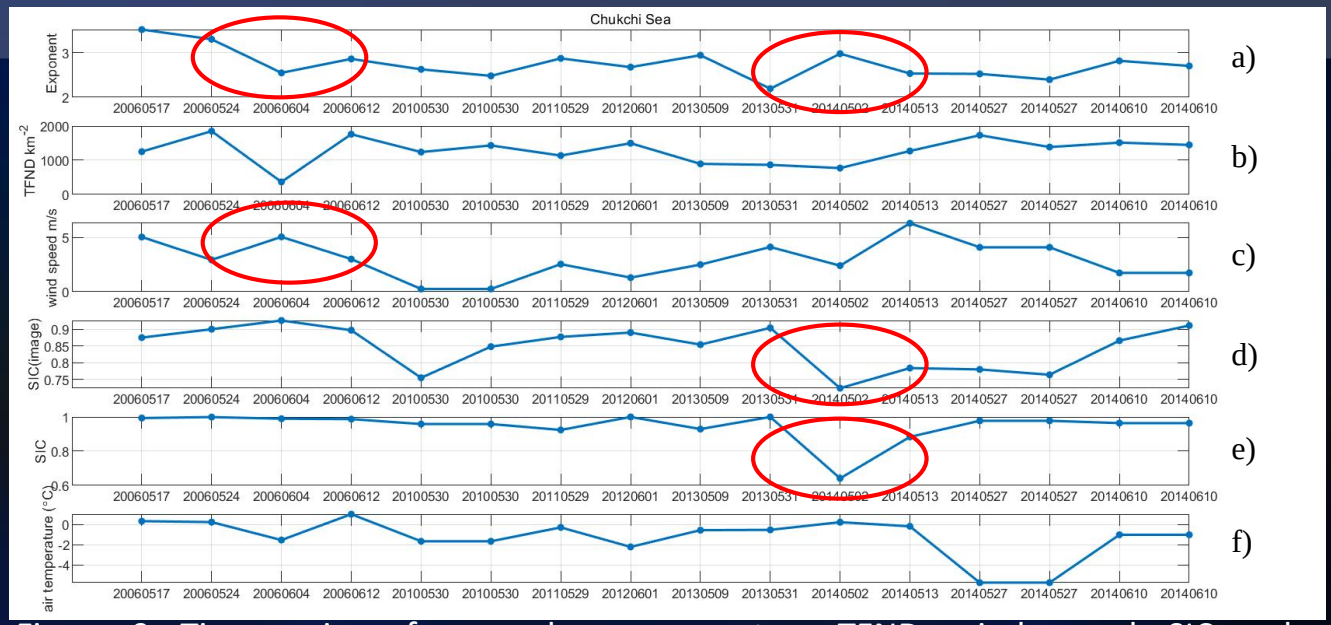

Figure 9. Time series of power-law exponent α, TFND, wind speed, SIC and air temperature. Panels (d) is the SIC from MEADEA image. Panels (e) shows the daily NOAA/NSIDC SIC data, AMSR-E and AMSR-2 SIC data.

- There is a **statistically significant correlation between α and air temperature in Chukchi Sea** (Fig. 8d), with the correlation coefficient of 0.67 at the 99% confidence level.
- The majority of α are not associated with wind speed or SIC in Chukchi Sea.
- However, some occasions, e.g. the data marked in red oval, show that the increase in α coincided with decrease in SIC and increase in wind speed (Fig. 9).

Results 4: Processes controlling regional FSD (East Siberian Sea)

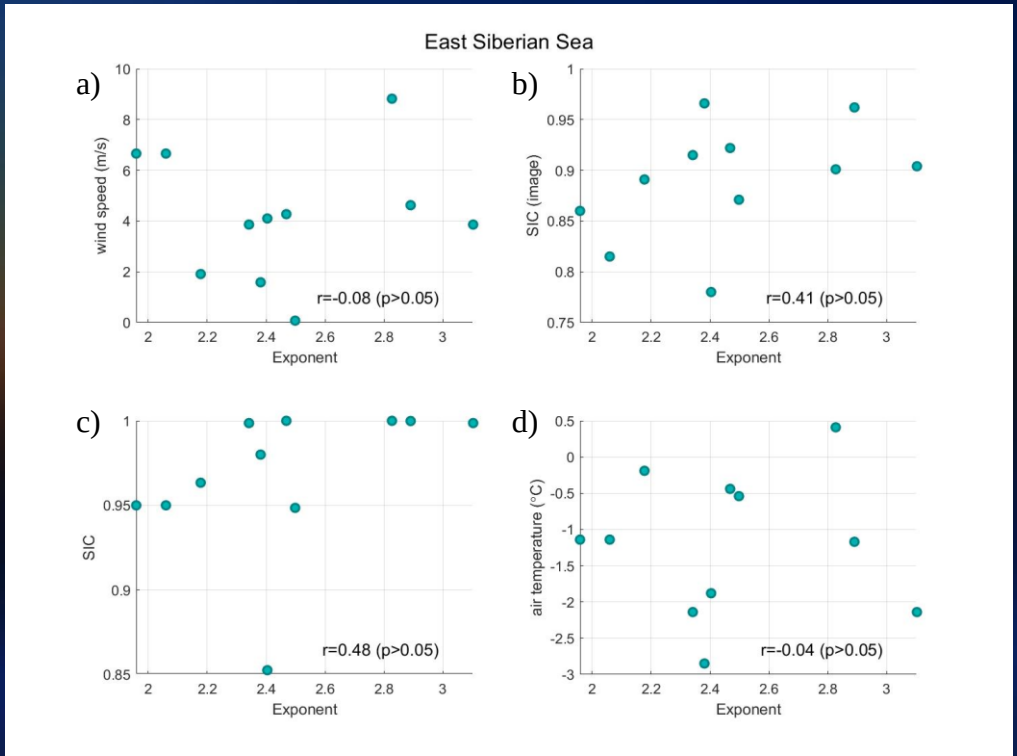

Figure 10. Correlation between the power-law exponent α and wind speed (a), SIC (b and c) and air temperature (d) in the East Siberian Sea. Panels (b) is the SIC from MEADEA image. Panels (c) shows the daily NOAA/NSIDC SIC data (2000-2001) and daily AMSR-E and AMSR-2 SIC data (2002, 2008, 2013 and 2014).

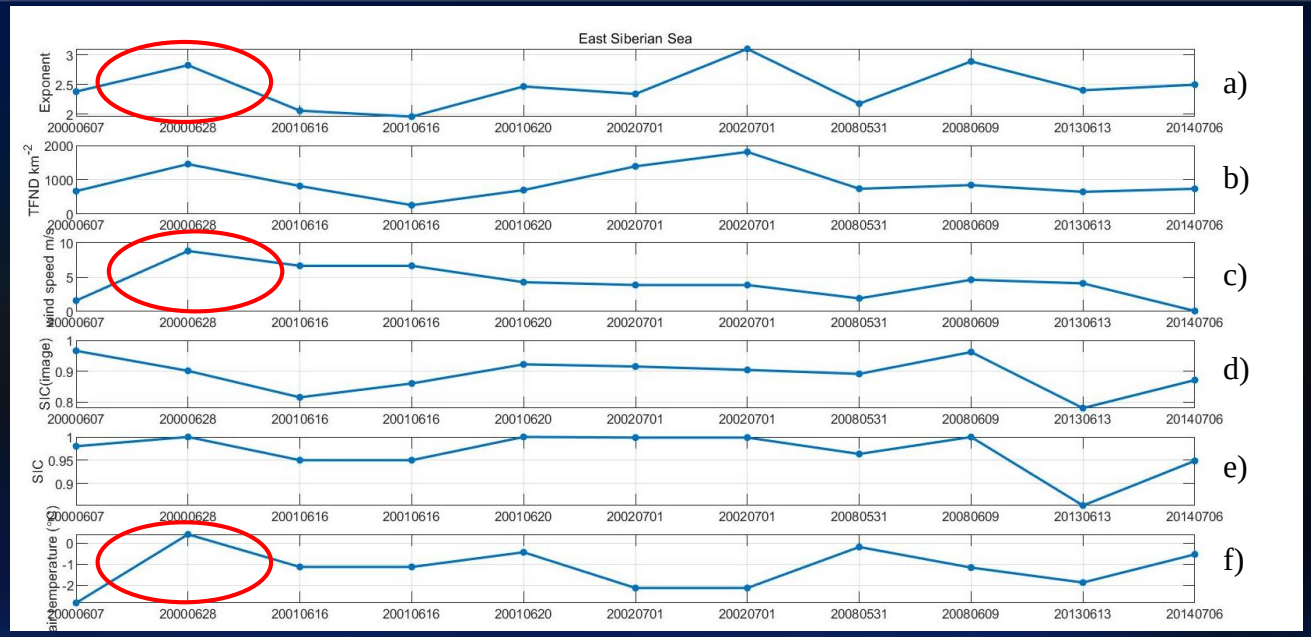

Figure 11. Time series of power-law exponent α, TFND, wind speed, SIC and air temperature. Panels (d) is the SIC from MEADEA image. Panels (e) shows the daily NOAA/NSIDC SIC data, AMSR-E and AMSR-2 SIC data.

- The majority of α are not associated with the wind speed, SIC or air temperature in East Siberian Sea (Fig. 10 and 11).
- However, one occasion in 2000 (Fig. 11 marked in red oval) shows that the increase in α coincided with increase in wind speed and air temperature.

Results 4: Processes controlling regional FSD (Fram Strait)

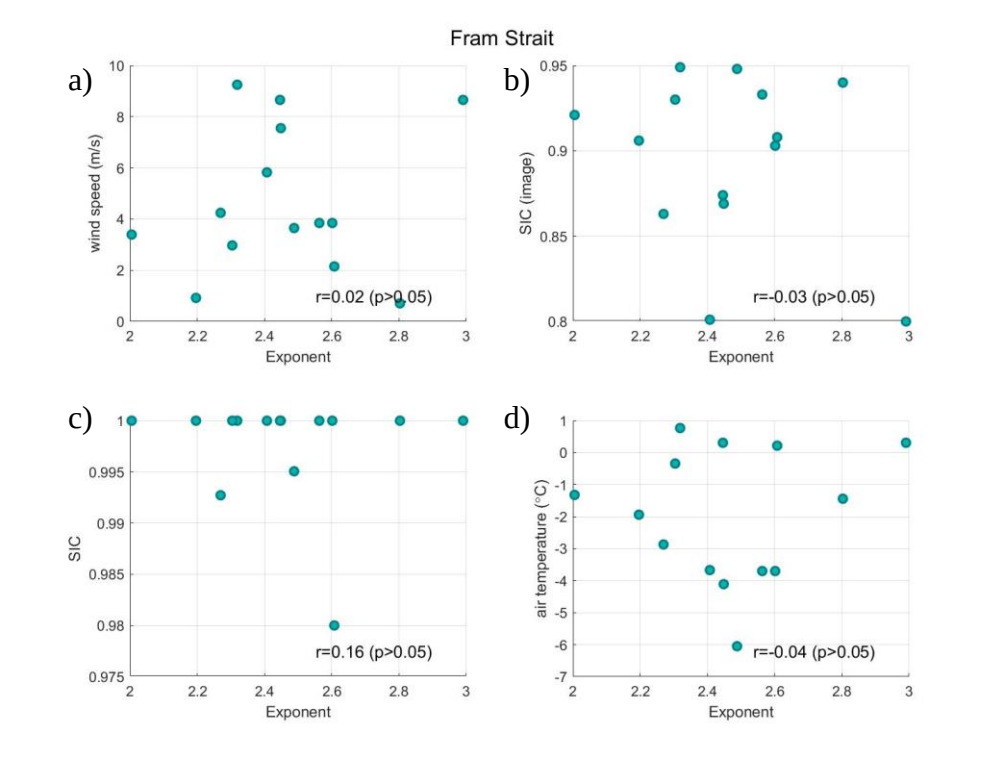

Figure 12. Correlation between the power-law exponent α and wind speed (a), SIC (b and c) and air temperature (d) in the Fram Strait. Panels (b) is the SIC from MEADEA image. Panels (c) shows the daily NOAA/NSIDC SIC data(2000-2001 and 2012) and daily AMSR-E and AMSR-2 SIC data (2002, 2009, 2013 and 2014).

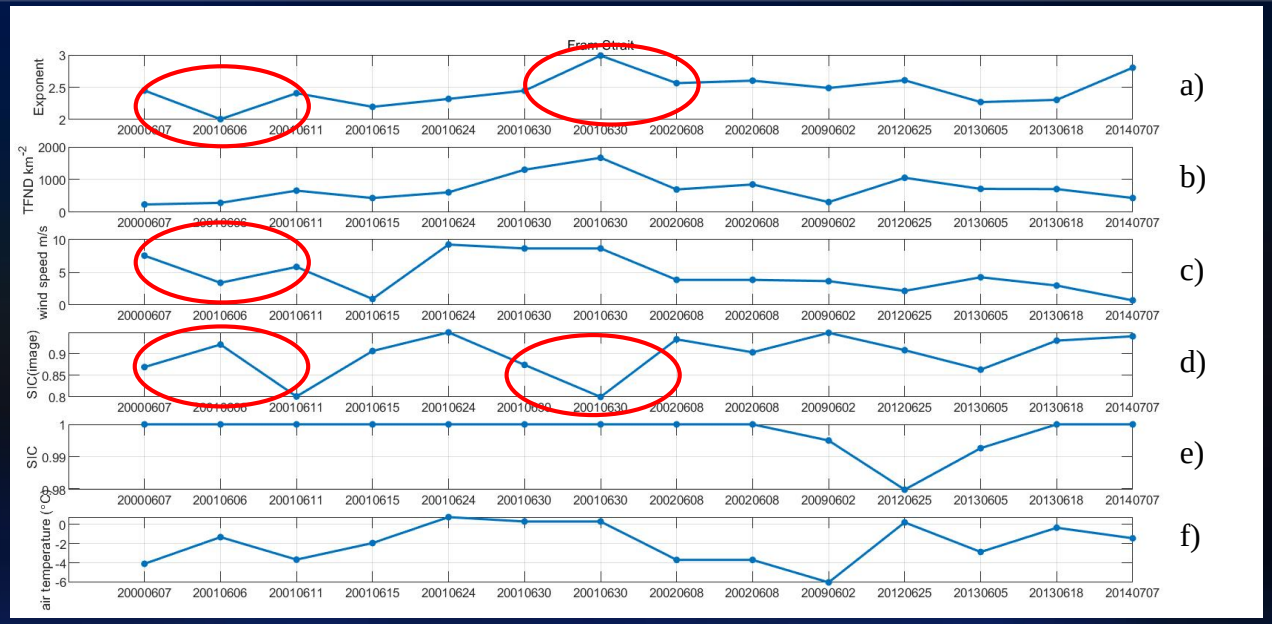

Figure 13. Time series of power-law exponent α, TFND, wind speed, SIC and air temperature. Panels (d) is the SIC from MEADEA image. Panels (e) shows the daily NOAA/NSIDC SIC data, AMSR-E and AMSR-2 SIC data.

- The majority of α are not associated with the wind speed, SIC or air temperature in Fram Strait (Fig. 12 and 13).
- However, some occasions, e.g. the data marked in red oval, shows that the change in α coincided with change in SIC and wind speed (Fig. 13).

Summary

- Chukchi Sea has the most variable and the largest percentage of small floes. Small floes increase 23% after 2012. The FSD is highly associated with the change of the air temperature. There is no correlation between FSD and wind speed and SIC in Chukchi Sea.
- In East Siberian Sea, there are less small floes compared with Chukchi Sea. Small floes has decreased by almost half across 2012. The FSD are not associated with the wind speed, SIC or air temperature in Fram Strait.
- In Fram Strait, the small floe is the least and its variability is relatively small. The change of FSD are not associated with the wind speed, SIC and air temperature. There is no significant change of FSD across 2012.

Discussion and future direction

No clear evidence for the change of FSD is associated with wind speed, SIC and air temperature in East Siberian Sea and Fram Strait

- In this study, the results are only from pre-ponding period (from late May to June), showing no major melt ponding. This means the thermodynamic processes are not sufficient to the change of FSD in this period.
- Limited number of data. Data are spare in spatial and temporal coverage.
- Image resolution was degraded to 2 meters. Currently re-processing FSD data at full-resolution (1 meter) to resolve small floes better.

Future Direction

- To derive and analyse more FSD data including post-ponding MEDEA images and other high-resolution satellite (e.g., Worldview) images
- To analyse how wave condition modifies the FSD in these 3 sites;
- To identify the key processes leading to regionally difference of FSD during melt season.

Reference

Hwang, B., Wilkinson, J., Maksym, E., Graber, H. C., Schweiger, A., Horvat, C., … Wadhams, P. (2017). Winter-to-summer transition of Arctic sea ice breakup and floe size distribution in the Beaufort Sea. *Elem Sci Anth*, *5*, 40. doi: 10.1525/elementa.232

Kwok R , & Untersteiner N. (2011). New High-Resolution Images of Summer Arctic Sea Ice. *EOS Transactions American Geophysical Union, 92(7)*, 53-54. doi: 10.1029/2011EO070002

Rothrock, D. A., & Thorndike, A. S. (1984). Measuring the sea ice floe size distribution. *Journal of Geophysical Research*, *89*(C4), 6477. doi: 10.1029/JC089iC04p06477

Virkar, Y., & Clauset, A. (2014). Power-law distributions in binned empirical data. *The Annals of Applied Statistics*, *8*(1), 89–119. doi: 10.1214/13-AOAS710